CHAPTER IV
RESULTS AND DISCUSSION

In this chapter, the results and discussion for the experiments are divided into four parts, namely, response-time experiment, batch adsorption experiment, no adsorption experiment, and fluidized-bed adsorption experiment.

4.1 Response Time Experiment

Figure 4.1 shows the comparison of the experimental and modeled response times by measuring the hydrogen concentration using an initial concentration of 0.4 N in a batch system with a mixing rate of 750 rpm. By fitting Equation 2.9 to the data, the response time constant of 0.1633 s^{-1} was obtained.

Figures 4.2, 4.3, and 4.4 compare the experiments and model by measuring the hydrogen concentration with the initial HCl concentration of 0.4 N in the fluidized-bed column with flow rates of 1.67, 2.17 and 2.5 ml/s, respectively. The response-time constants according to this model are shown in Table 4.1. The results show that the response time constant depends on the flow rate. The higher flow rate of the feed solution, the more quickly the process reach in equilibrium.

Table 4.1 The effect of flow rate on the response time constant

Flow rate(ml/s)	Response time constant (s^{-1})
1.67	0.085
2.17	0.1291
2.50	0.1303

4.2 Batch Operation

Figure 4.5 shows the concentration of desorbed hydrogen ions for different cationic salts, namely, Ca^{2+}, Mg^{2+} and Na^{+} with the total initial concentration of each cationic salt being 0.2 N. From the experimental results, the rate of hydrogen ion desorbed from the resin decreases from the highest for Ca^{2+}, through an intermediate value for Mg^{2+}, to the lowest for Na^{+}. The results show that the extent of the exchange increases with increasing *valence* of the exchanging ion and with increasing *atomic number* of the exchanging ion if the valence is constant.

Figure 4.6 shows the concentration of desorbed hydrogen ions for the mixed-ion solution of Ca^{2+} and Mg^{2+} with the total initial concentration being 0.2 N. The rate of hydrogen ions desorbed from the resin is lower than that of Ca^{2+} and Mg^{2+}, individually. This is because of the decrease of *atomic number* of the exchanged ion. Also, the result shows that the rate of hydrogen ion exchange with Ca^{2+} is higher than Mg^{2+} in the mixed-ion solution.

Figure 4.7 shows the amounts of cations adsorbed on the resin (q) as a function of time for various cations. The experiment shows that the equilibrium concentration of Ca^{2+} in the resin phase (q_e) is higher than that of Mg^{2+}, which, in turn, is higher than that of Na^{+}. Also in the mixed-ion solution, the equilibrium concentration of Ca^{2+} in the resin phase (q_e) is higher

than that of Mg^{2+}. The results also show the resin preferentially adsorbs more Ca^{2+} than Mg^{2+}.

Figures 4.8 to 4.13 compare the experimental rates of adsorption with those predicted by the theory, for the batch operation. According to the model, the proposed equation for the rate of adsorption is shown in Equation 2.16. From Equation 2.21, the Excel solver application was employed to solve for the model parameters, which are given in Table 4.2.

Table 4.2 Model parameters in the batch operation with different solutions

Solution	q_t (meq/ml)	k_1 (s^{-1})	k_2
NaCl	1.130	0.170	0.377
$CaCl_2$	1.130	0.237	2.161
$MgCl_2$	1.130	0.217	1.295
Mixed-ion solution of Ca^{2+} and Mg^{2+}	1.130	0.165	0.850
Ca^{2+} in Mixed-ion solution of Ca^{2+} and Mg^{2+}	1.130	0.163	0.320
Mg^{2+} in mixed-ion solution of Ca^{2+} and Mg^{2+}	1.130	0.119	0.313

According to Table 4.2, the rate constants (k_1) for the batch experiments with $CaCl_2$, $MgCl_2$, NaCl and the mixed-ion solution of Ca^{2+} and Mg^{2+} are 0.237, 0.217, 0.165, 0.006, and 0.005 s^{-1}, respectively. The results show that, with the highest k_1, the exchange rate of Ca^{2+} is faster than that of Mg^{2+}, which, in turn, is higher than that of Na^{2+}. Also in the mixed-ion solution, the exchange rate of Ca^{2+} is faster than that for Mg^{2+}. Accordingly, the rate of exchange depends on the particular cation being adsorbed. Next, the equilibrium constants (k_2) of these experiments for $CaCl_2$, $MgCl_2$, NaCl and the mixed-ion solution of Ca^{2+} and Mg^{2+} with the total initial concentration 0.2 N. are 2.161, 1.295, 0.377 and 0.850, respectively. These values show that the exchanger has the strongest preference for Ca^{2+}. In the

mixed-ion solution, the equilibrium constant (k_2) for Ca^{2+} is 0.320, which is almost the same as that for Mg^{2+}. The result also implies that the exchanger is equally favorable to Ca^{2+} and Mg^{2+} with a total initial concentration of 0.2 N. Lastly, the best-fit parameter shows that the total exchange capacity (q_t) (the total concentration of cations) is 1.13 meq /ml.

4.3 No Adsorption in Fluidized-Bed Ion-Exchange Column

From the model, the analytical solution of Equations 2.18 to 2.20 gives the hydrogen ion concentration leaving the CSTR and PFR. Moreover, the response time constant (α_e) obtained from the previous experiment was inserted into Equation 2.22 in order to find the hydrogen concentration (h_p) leaving the PFR. Also, the void fraction, when the bed is fluidized, was used in Equation 2.7. The experimental conditions in the no adsorption experiment were v = 1.67 ml/s, V_L = 78.69 ml, V_R = 48.95 ml and h_o = 0.40 meq/ml.

For the case of no adsorption, the experimental results are compared with those predicted by three different models, as follows:

1. Figure 4.14: one CSTR and one PFR in series.
2. Figure 4.15: two CSTRs and one PFR in series.
3. Figure 4.16: three CSTRs and one PFR in series.

The results show that the best fit between the theory and experiment is obtained when the model accounts for just one CSTR in series with one PFR. By fitting model with the experimental data, the sum squared of the experimental data and model by measured the hydrogen ion concentration $SUM(h_m(exp)-h_m(model))^2$ is 0.0267, 0.0327 and 0.0499 compared to one CSTR and one PFR in series, two CSTRs and one PFR in series and three CSTRs and one PFR in series, respectively. Therefore, such a model will be used in the subsequent investigation of adsorption.

4.4 Adsorption in Fluidized-Bed Exchange Column

Figures 4.17- 4.22 compare the experimental and theoretical values of the hydrogen concentration leaving the PFR in an adsorption operation. The experimental conditions are shown in Table 4.3.

Table 4.3 The experimental conditions with adsorption in the fluidized-bed column

Condition	$CaCl_2$	$MgCl_2$	NaCl	Mixed-ion solution
V(ml/s)	1.67	1.67	1.67	1.67
V_L(ml/s)	83.40	79.88	105.08	117.84
c_o(meq/ml)	0.20	0.20	0.20	0.20
q(meq/ml)	1.13	1.13	1.13	1.13
α_e	0.085	0.085	0.085	0.085

The results show that there is no hydrogen concentration initially (t = 0). When the solution passes through, the cations in the solution are exchanged for the hydrogen ions in the resin. The solution is more concentrated with hydrogen ions and dilute in different cationic salts, namely, calcium ions, magnesium ions, sodium ions and mixed calcium and magnesium ions as shown in Figures 4.17. As the resin becomes saturated, the desorption of hydrogen ions declines. Eventually, equilibrium is reached and further exchange ceases.

From the model, the solution of the governing equations was used and the values of the rate constant (k_1) and equilibrium constant (k_2) were found by minimizing the sum of squares of the deviation between the hydrogen concentration data in solution and hydrogen concentration predicted by the model. It should be mentioned that the governing equations were solved with

a numerical approximation in an Excel spreadsheet. Furthermore, the values of constant are shown in Table 4.4

Table 4.4 Summary of the rate and equilibrium constants in the fluidized-bed operation

Solution(0.2N)	$k_1(s^{-1})$	k_2
$CaCl_2$	0.009	24.99
$MgCl_2$	0.0073	19.00
NaCl	0.0049	14.01
Mixed-ion solution	0.0063	18.00
Ca^{2+} in mixed-ion solution	0.0044	10.00
Mg^{2+} in mixed-ion solution	0.0039	8.90

The value of the rate constant (k_1) progresses from high to low through the following sequence: calcium ions (highest), magnesium ions, mixed-ion solution of calcium ions and magnesium ions, sodium ions, calcium ions in mixed-ion solution, and magnesium ions in mixed-ion solution (lowest). These values imply that the exchange rate of calcium ions in the solution with hydrogen ions on the resin is the fastest. This is because the pore diffusion rate, which is important in adsorption, depends on the selectivity of the exchanger, which prefers the higher valence of the exchanging ion and the higher atomic number of the exchanging ion if the valence is constant. In the mixed-ion solution, the transfer of calcium ions is also preferred to that of magnesium ions, for which the trends of these results are the same as shown in batch experiments.

When comparing the rate constant (k_1) in the fluidized bed and batch operations, the rate constant in the batch operation is higher than the fluidized-bed column, because of the higher stirrer speed and good mixing in the batch

operation. So the film diffusion is important to the rate of adsorption in the fluidized-bed operation.

The value of the equilibrium constant (k_2) progresses from high to low through the following sequence: calcium ions (highest), magnesium ions, mixed-ion solution of calcium ions and magnesium ions, and sodium ions (lowest) because the equilibrium is merely related to the selectivity of the exchangers.

When comparing the equilibrium constant (k_2) in the fluidized bed and batch operation, the equilibrium constant in the batch operation is less than in the fluidized-bed column because the operation in the fluidized-bed mode acts as many batchwise stages.

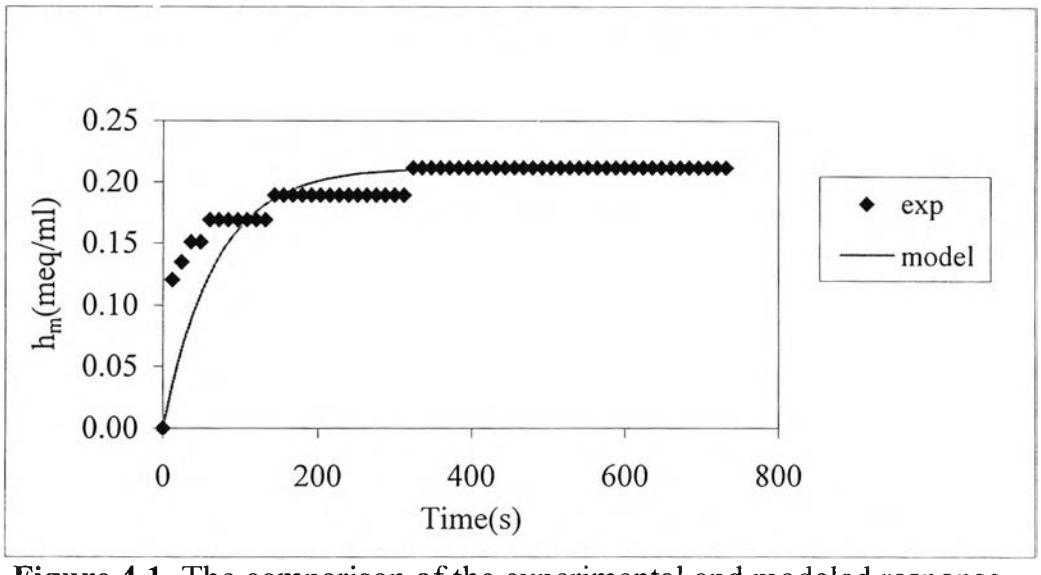

Figure 4.1 The comparison of the experimental and modeled response times by measuring the hydrogen concentration in a batch system with mixing rate of 750 rpm

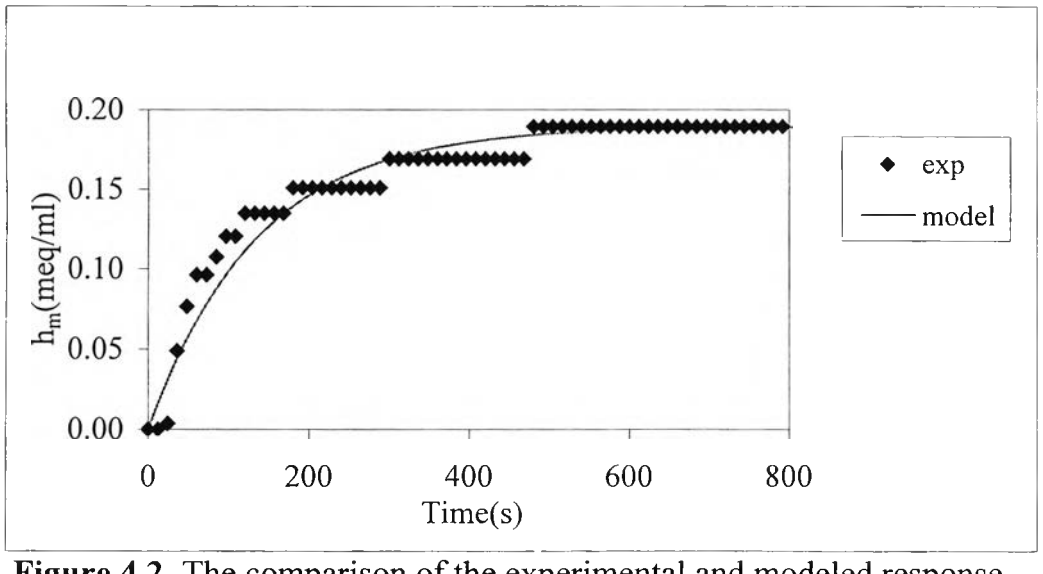

Figure 4.2 The comparison of the experimental and modeled response times by measuring the hydrogen concentration in the fluidized-bed column with flow rate of 1.67 ml/s

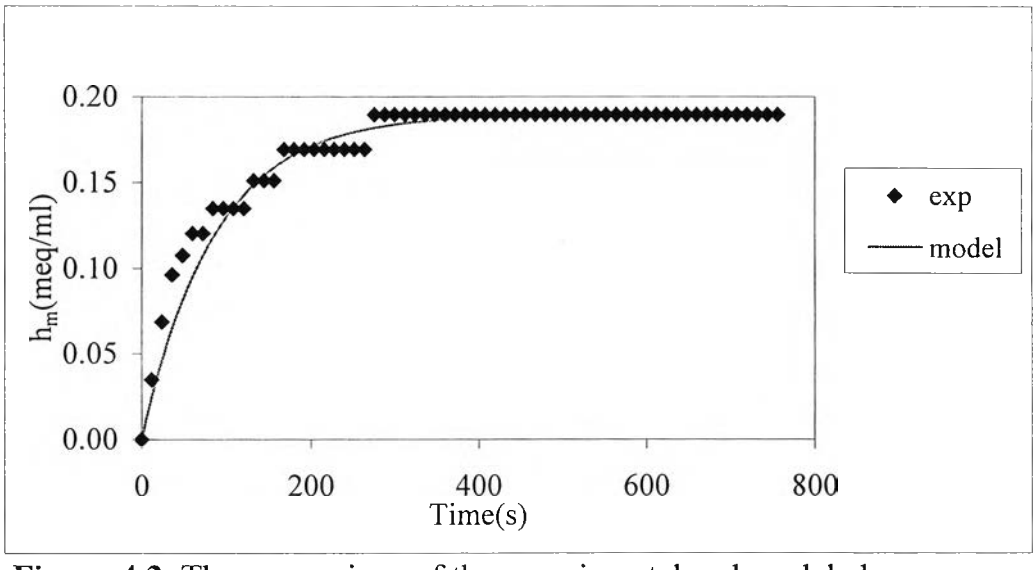

Figure 4.3 The comparison of the experimental and modeled response times by measuring the hydrogen concentration in the fluidized-bed column with flow rate of 2.17 ml/s

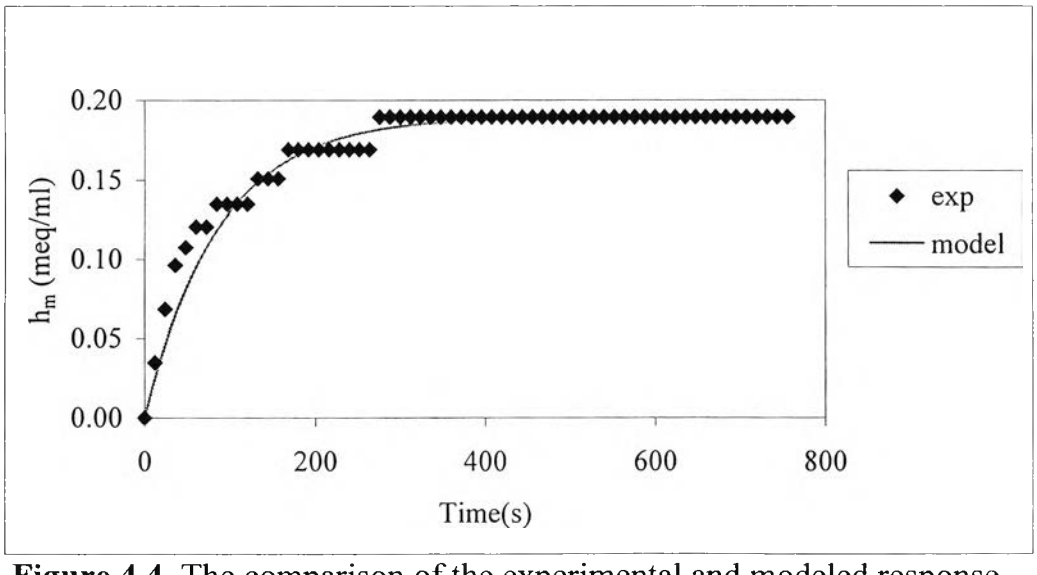

Figure 4.4 The comparison of the experimental and modeled response times by measuring the hydrogen concentration in the fluidized-bed column with flow rate of 2.5 ml/s

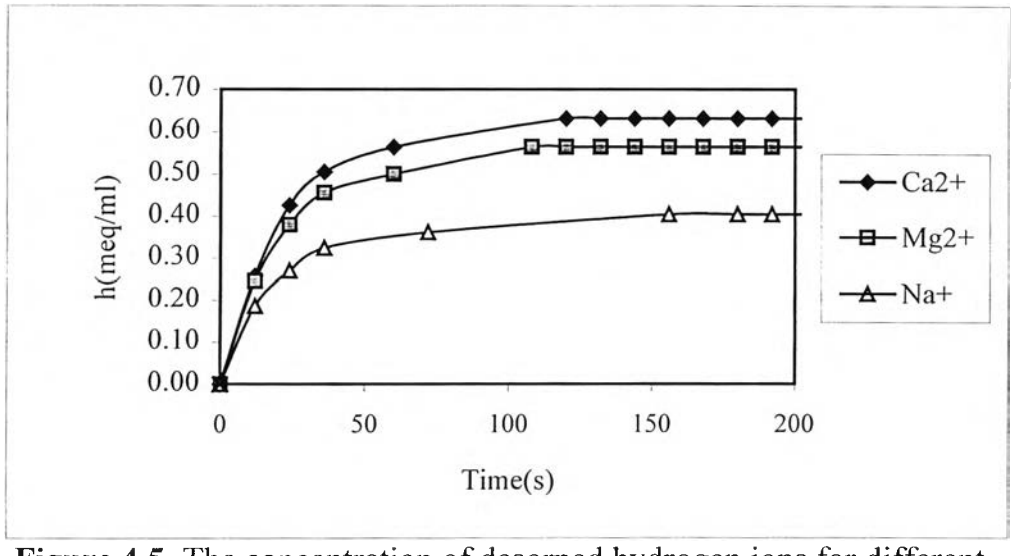

Figure 4.5 The concentration of desorped hydrogen ions for different cationic salts with the total initial concentration 0.2 N

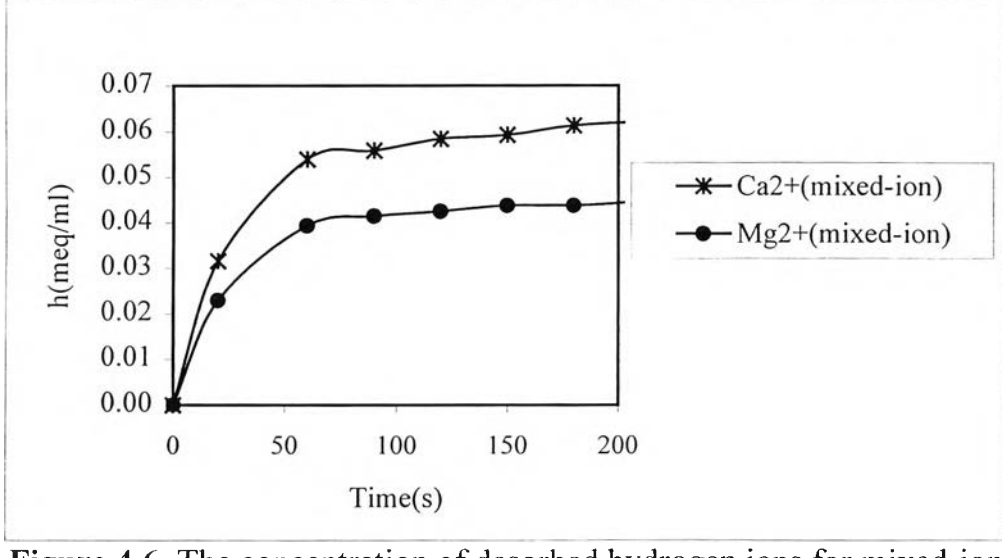

Figure 4.6 The concentration of desorbed hydrogen ions for mixed-ion solution of Ca^{2+} and Mg^{2+} with the total initial concentration 0.2 N.

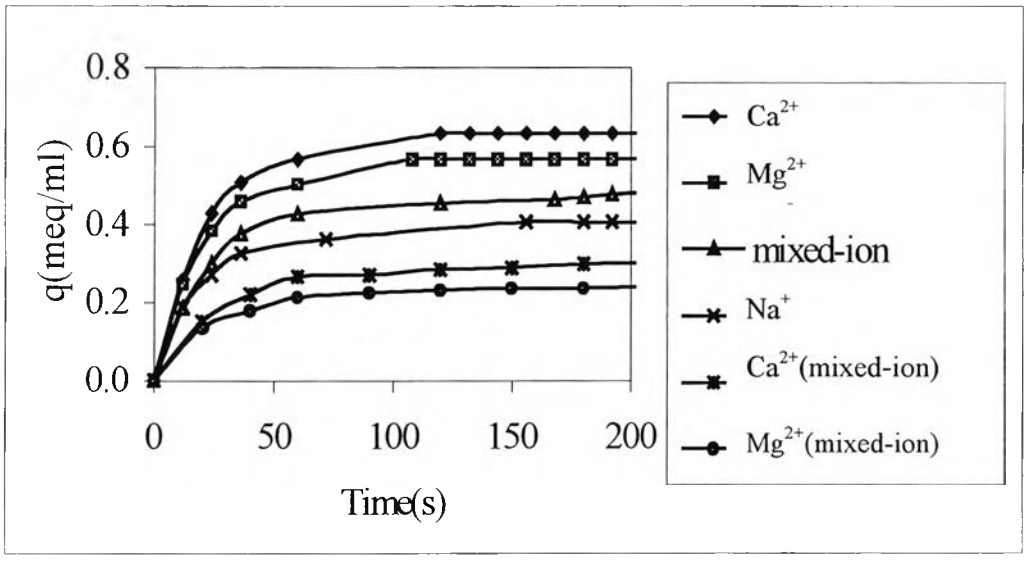

Figure 4.7 The cation adsorbed on the resin (q) as a function of time for various cationic salts

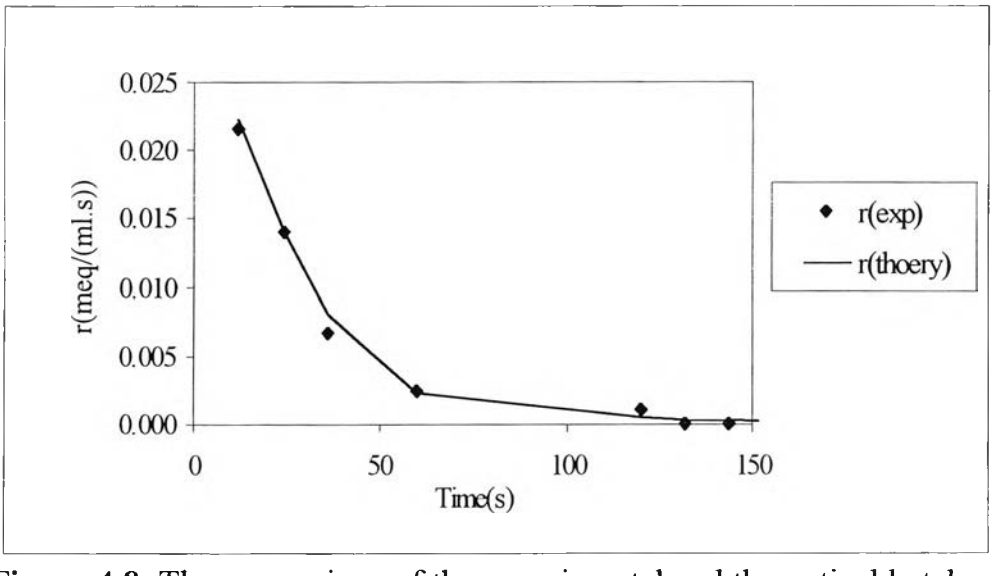

Figure 4.8 The comparison of the experimental and theoretical batch adsorption rates for Ca^{2+}

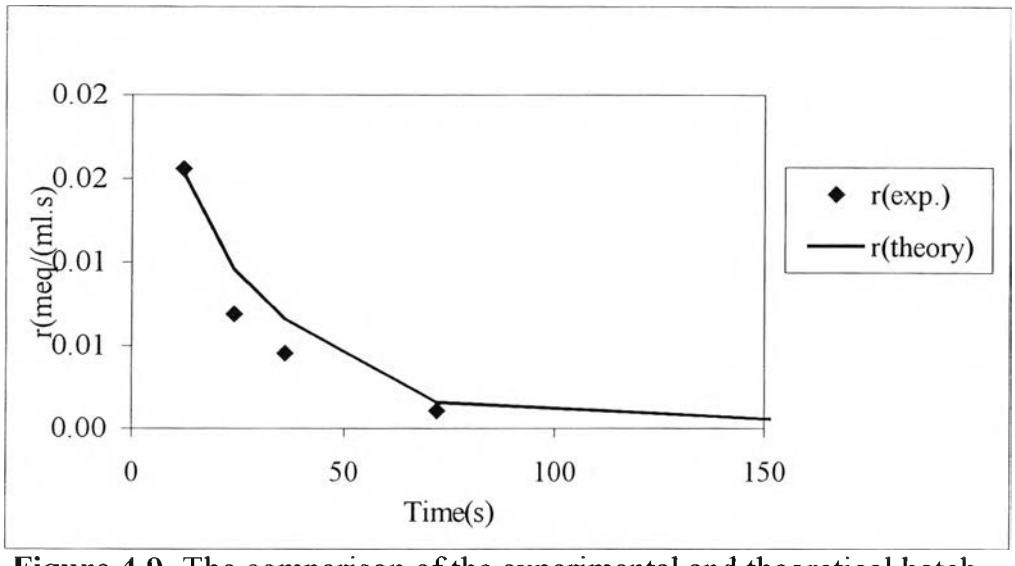

Figure 4.9 The comparison of the experimental and theoretical batch adsorption rates for Mg2+

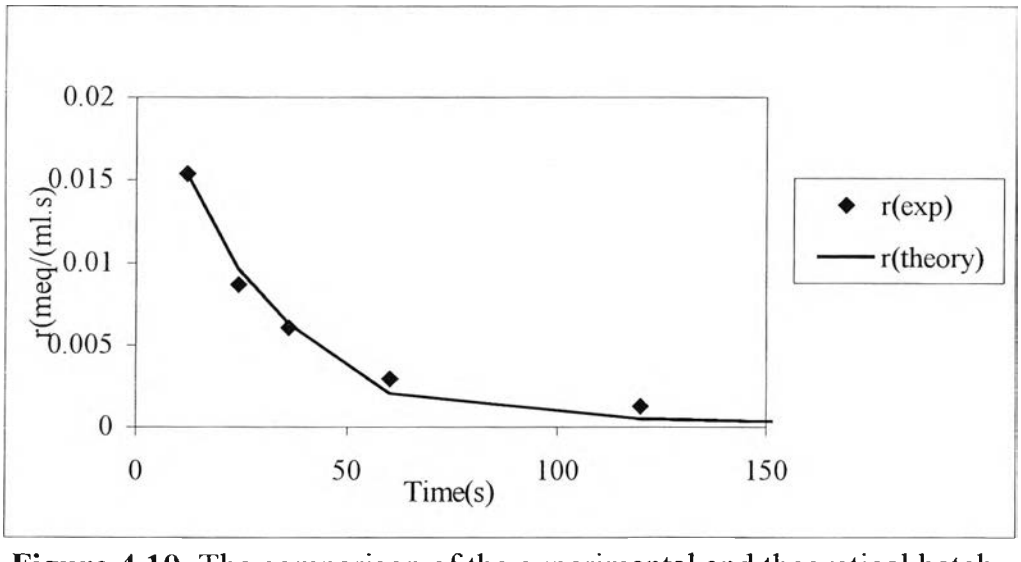

Figure 4.10 The comparison of the experimental and theoretical batch adsorption rates for Na^{+}

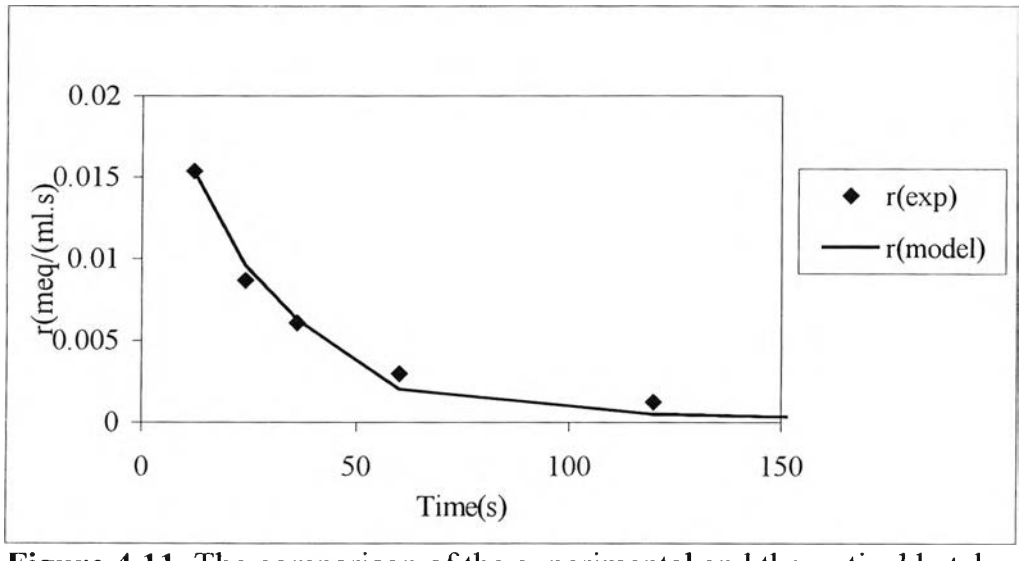

Figure 4.11 The comparison of the experimental and theoretical batch adsorption rates for mixed-ion of Ca^{2+} and Mg^{2+}

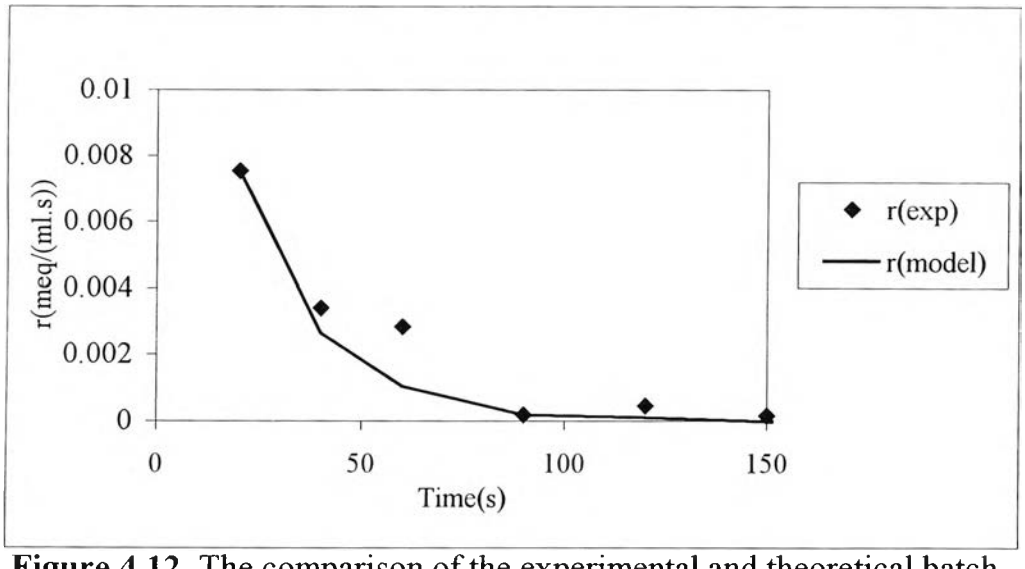

Figure 4.12 The comparison of the experimental and theoretical batch adsorption rates for Ca^{2+} in mixed-ion solution

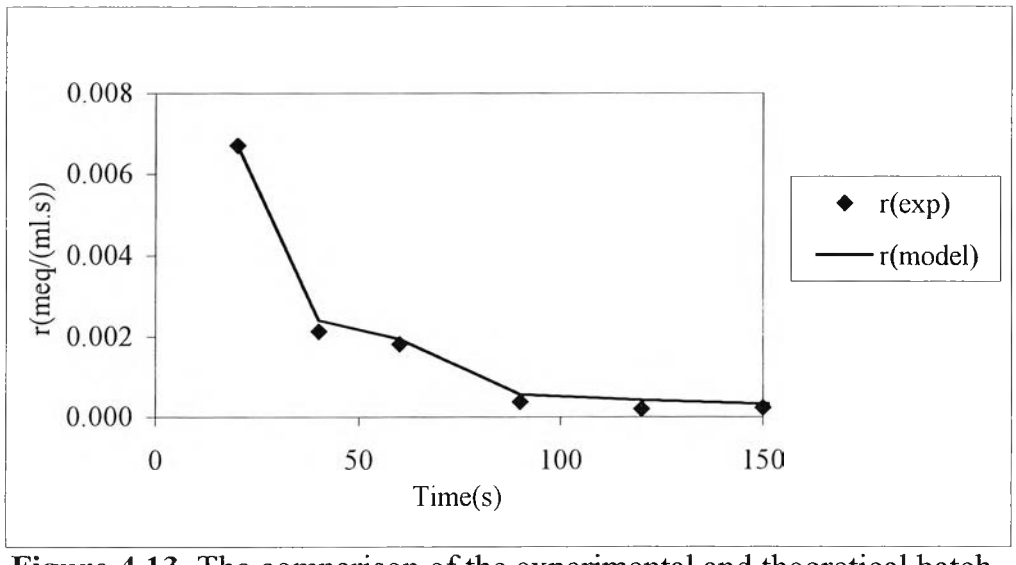

Figure 4.13 The comparison of the experimental and theoretical batch adsorption rates for Mg^{2+} in mixed-ion solution

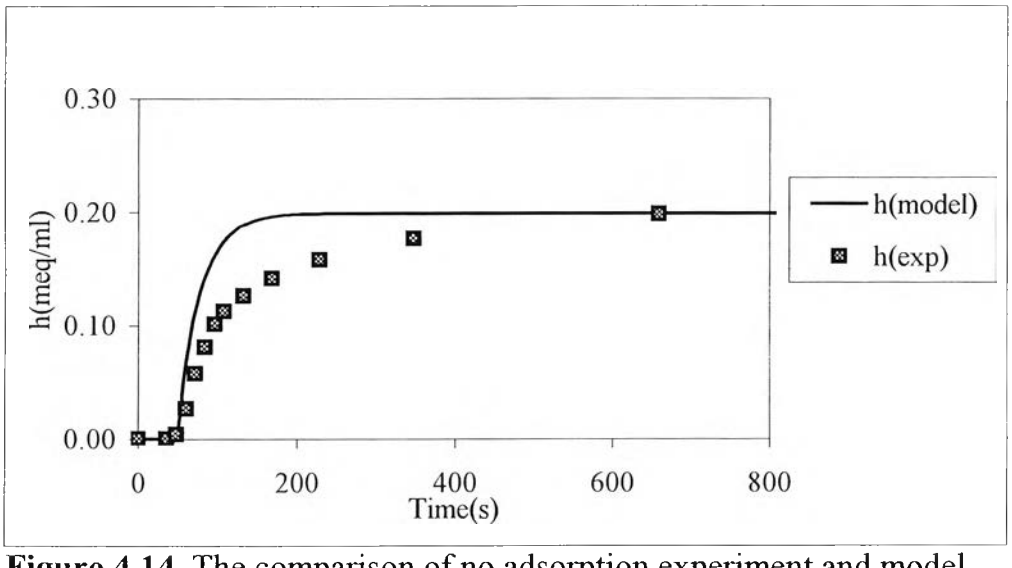

Figure 4.14 The comparison of no adsorption experiment and model with one CSTR and one PFR in series

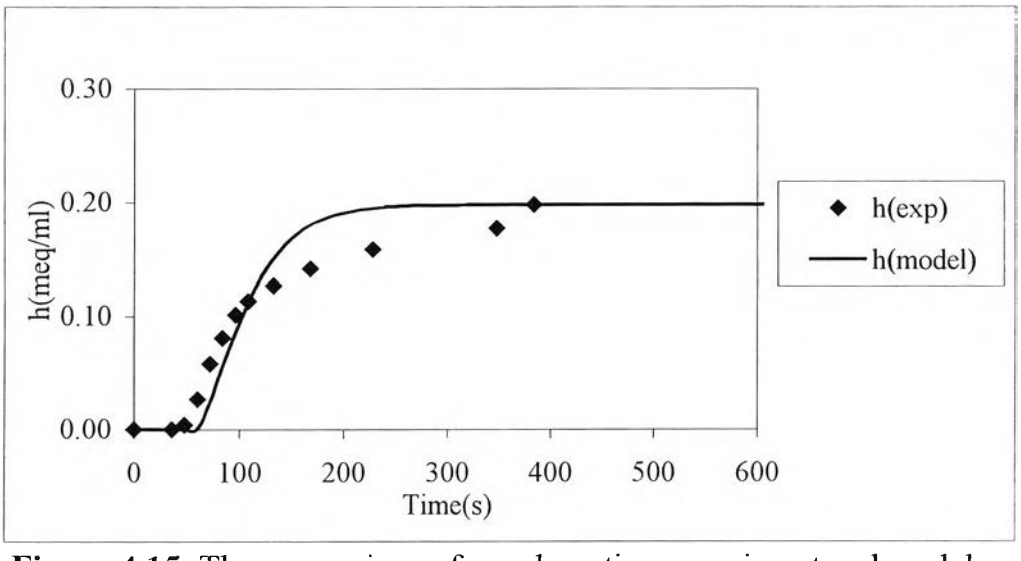

Figure 4.15 The comparison of no adsorption experiment and model with two CSTRs and one PFR in series

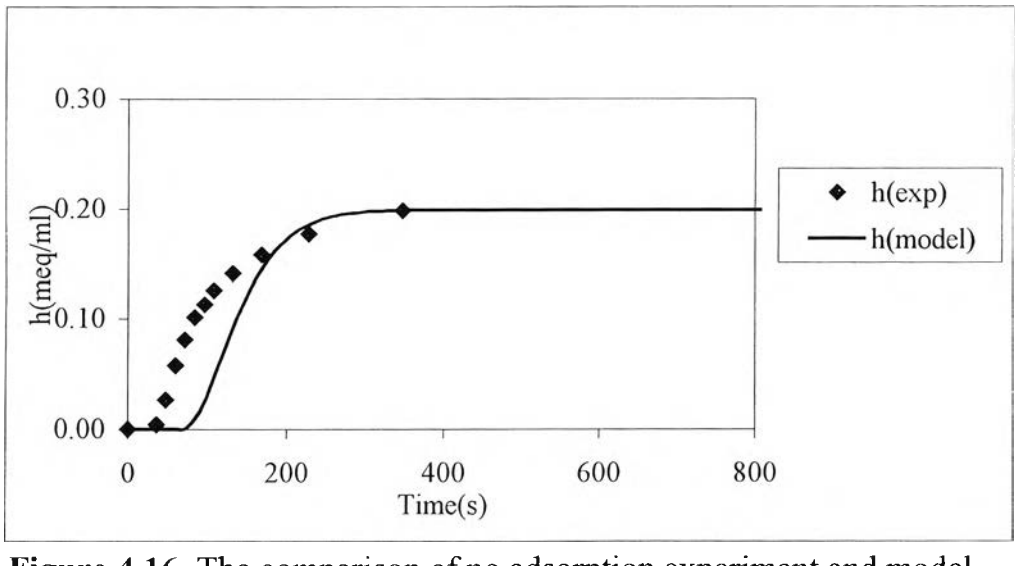

Figure 4.16 The comparison of no adsorption experiment and model with three CSTRs and one PFR in series

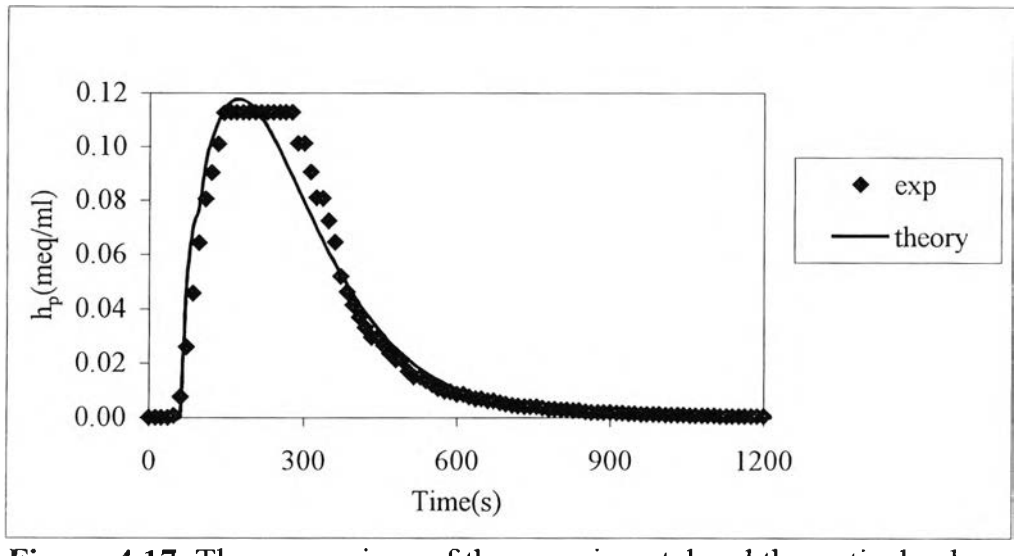

Figure 4.17 The comparison of the experimental and theoretical values of the hydrogen concentration leaving the PFR in an adsorption operation with $CaCl_2$

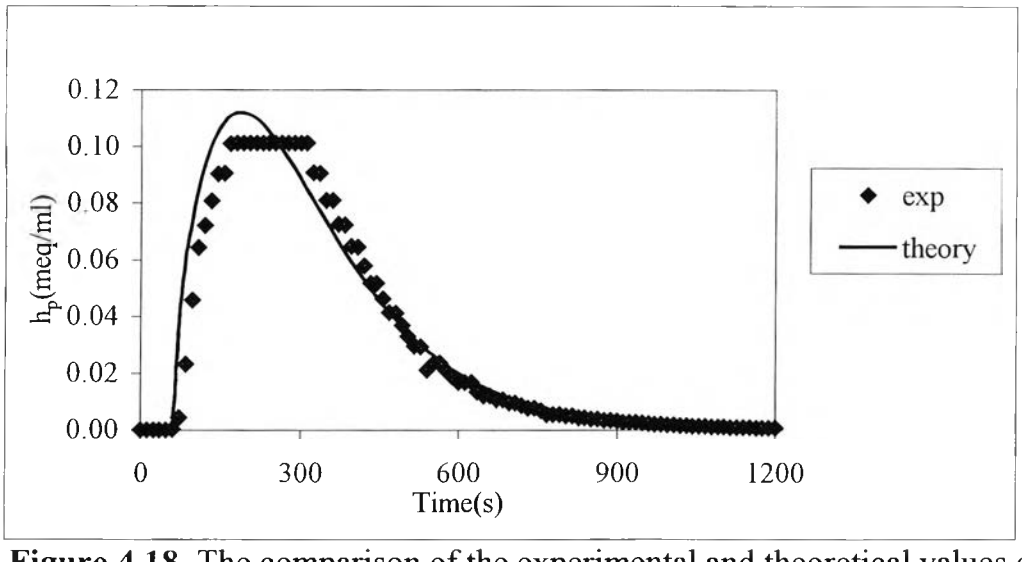

Figure 4.18 The comparison of the experimental and theoretical values of the hydrogen concentration leaving the PFR in an adsorption operation with $MgCl_2$

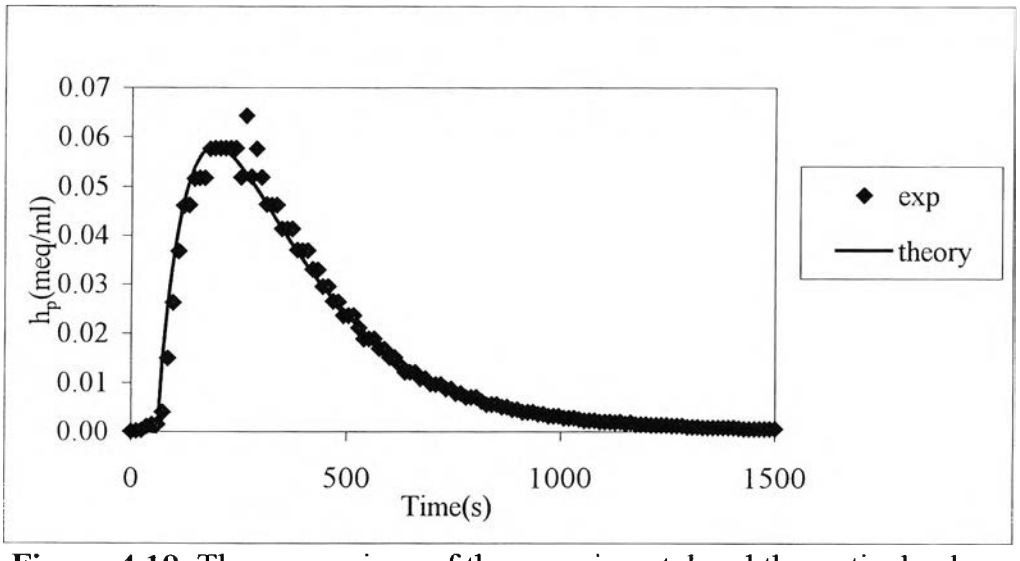

Figure 4.19 The comparison of the experimental and theoretical values of the hydrogen concentration leaving the PFR in an adsorption operation with NaCl

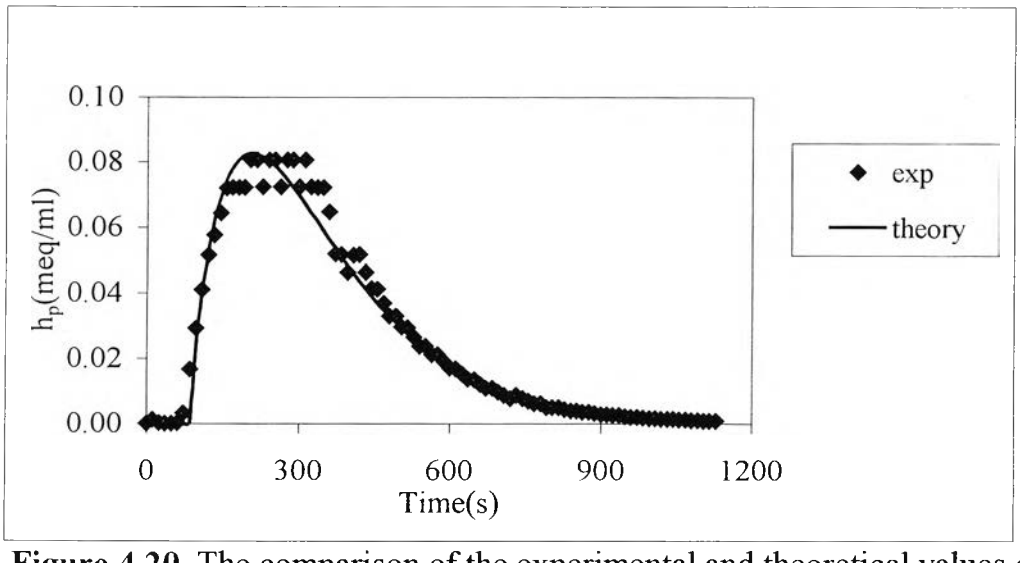

Figure 4.20 The comparison of the experimental and theoretical values of the hydrogen concentration leaving the PFR in an adsorption operation with mixed-ion solution of Ca^{2+} and Mg^{2+}

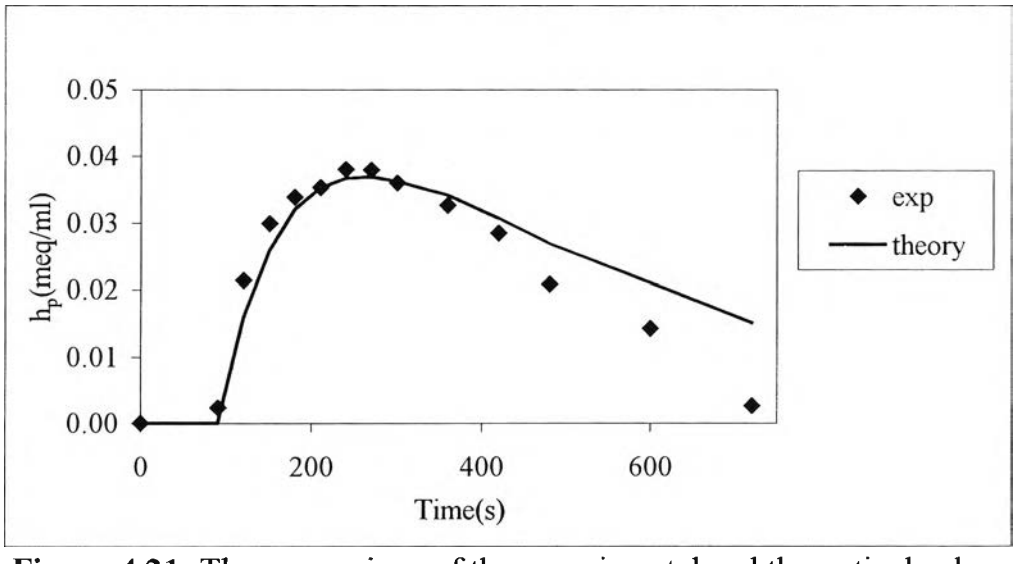

Figure 4.21 The comparison of the experimental and theoretical values of the hydrogen concentration leaving the PFR in an adsorption operation with Ca^{2+} in mixed-ion solution

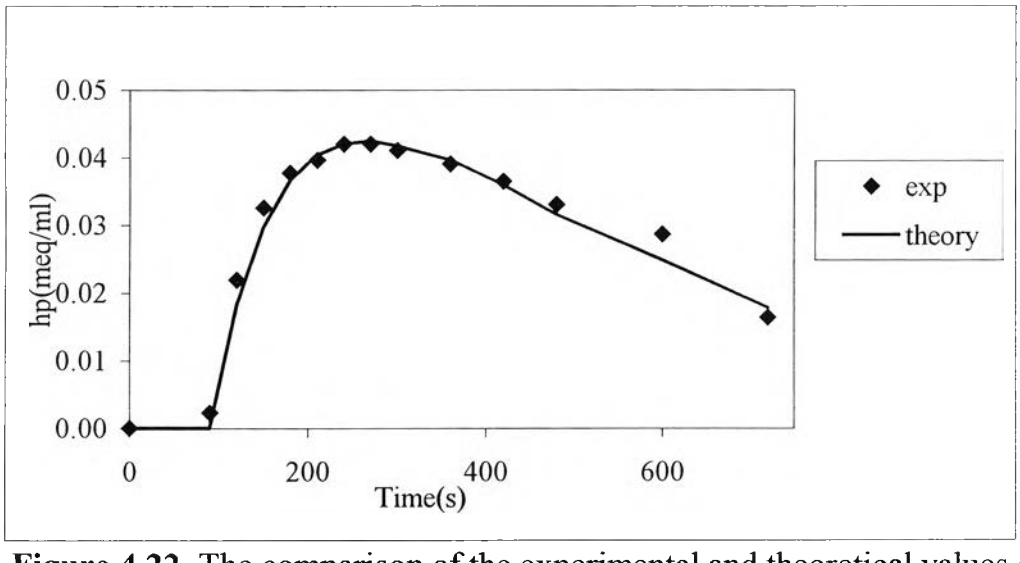

Figure 4.22 The comparison of the experimental and theoretical values of the hydrogen concentration leaving the PFR in an adsorption operation with Mg^{2+} in mixed-ion solution